



RESEARCH PAPER

OPEN ACCESS

**Petrogenesis of mafic meta volcanic rocks in NW Isfahan, Central Iran**

Zohreh Hossein Mirzaee\*, Ali-Khan Nasr-Esfahani<sup>1</sup>

*Young Researcher and Elite Club, Khorasgan (Isfahan) Branch, Islamic Azad University, Isfahan, Iran*

*<sup>1</sup>Geology department, Islamic Azad University, Isfahan (Khorasgan) Branch, Iran*

**Key words:** Metavolcanic, Neo-Tethyan, Petrology, Sanandaj-Sirjan.

Article published on January 31, 2015

**Abstract**

The study area is located in west of Isfahan, Shahrekord-Dehsard terrene. This area is the part of Sanandaj-Sirjan structural Zone. In this area, metamorphosed igneous outcrop contain of greenschist and meta volcanic rocks. These rocks have metmorphed in greenschist facies and belong to the age of Triassic- Jurassic. The Meta volcanic is mainly composed of plagioclase, amphibole, epidote and chlorite. Geochemical data shows that parent rocks are basalt to andesitic basalt composition with subalkaline and tholeiitic trend. In the REE and trace elements spider diagrams, these similar to MORB and adapted with E-MORB. These results indicated that meta volcanic generated back arc basin volcanic subduction environment. Meta volcanic in Sahrekord - Dehsard terrene shows remnants of Neo-Tethyan oceanic lithosphere with back arc basin environment that was subducted and uplifted to the surface.

**\*Corresponding Author:** Zohreh Hossein Mirzaee ✉ [zohreh.mirzaee@ymail.com](mailto:zohreh.mirzaee@ymail.com)

## Introduction

The Sanandaj-Sirjan Zone is thrust over the Arabian platform along the main Zagros Fault. The main Zagros Fault is deeply rooted and coincides with the suture between the Arabian plate and Sanandaj-Sirjan Zone. The main ambiguity on the tectonic evolution of the southeastern Zagros orogenic belt is the time when the Neo-Tethys oceanic crust disappeared completely between the central Iran micro continent and the Arabian plat. Based on this review, the subduction of the Neo-Tethys oceanic lithosphere has continued up to middle Miocene time and final collision between the Arabian plate and the central Iran micro continent occurred in the late micro continent. Once Neo-Tethys rifting occurred in the upper Carboniferous- lower Permian. In the upper Triassic- lower Jurassic Neo-Tethys under thrust in under central Iran micro continent. Arfania and Shahriari have suggested that Shahrekord-Dehsard consists two oceanic basins, Neo-Tethys 1 and Neo-Tethys 2. In this model the evolution of several stages, Subduction, Oceanic lithosphere and continental collision of upper Triassic to Pliocene. During the late Triassic- early Jurassic a new spreading ridge, the second Neo-Tethys, was created to separate the Shahrekord- Dehsard terrain. From Afro- Arabian plate and developed back arc basin. Simultaneously, the second Neo-Tethys spreading and primary Neo-Tethys closing occurred in the upper Miocene and late. Probably the upper Miocene-Pleistocene, second Neo-Tethys is completely closed.

The Zagros orogen as a part of the Alpine-Himalaya mountain chain is a well-defined active doubly-vergent and asymmetric orogenic belt (Alavi, 2004) and extends in a northwest-southeast direction for about 2000 km from the Taurus mountain of southeastern Turkey to the Bandar-Abas syntax in southern Iran ( Arfania & Shahriari, 2009). This orogenic belt (Fig. 1) consists of four NW-SE trending parallel zones: (1) Urumieh-Dokhtar Magmatic Arc (UDMA); (2) Sanandaj-Sirjan Zone (SSZ); (3) High Zagros; and (4) Zagros Simply Folded Belt (ZSFB).

The Sanandaj-Sirjan Zone (SSZ) is a narrow zone of highly deformed rocks located between the towns of Sirjan in the southeast and Sanandaj in the northwest (Mohajjel & Fergusson, 2000). The Sanandaj-Sirjan Zone is a metamorphic belt (greenschist amphibolite facies) that was exhumed during the Cretaceous-Tertiary continental collision between the Afro-Arabian continent and the Iranian plate (e.g., Sengor & Natalin, 1996, Mohajjel & Fergusson, 2000; Mohajjel *et al*, 2003). The rocks in this zone are the most highly deformed in the Zagros orogen and share the NW-SE trend of its structures. The Sanandaj-Sirjan Zone is thrust over the Arabian Platform along the Main Zagros Fault, which is marked at the surface by a discontinuous belt of ophiolitic rocks and mélanges running along the entire length of the orogen (Ricou, 1974). The Main Zagros Fault is deeply rooted and coincides with the suture between the Arabian Plate and Sanandaj-Sirjan Zone (Agard *et al*, 2005, Berberian, 1995). The Zagros Fold-Thrust Belt is a result of a total shortening of 65–78 km across the Zagros sedimentary basin from the Early Miocene onwards (Mouthereau *et al*, 2007). The basin is characterized by a sequence of sedimentary rocks up to 12 km thick including Paleozoic and Mesozoic shelf sediments and Cenozoic syn-orogenic strata that were deposited on the subsiding northeastern Arabian continental margin. In the Golpaygan area, the Sanandaj-Sirjan Zone can be subdivided into two parts: (i) southeastern part consisting of Jurassic metamorphosed rocks; and (ii) northwestern part, deformed in the Late Cretaceous, containing many intrusive felsic rocks (Eftekharijad, 1981). The southeastern Sanandaj-Sirjan Zone is subdivided transversally into two separate regions: (i) northeastern region (Esfahan-Sirjan Block) consisting of Paleozoic, Mesozoic, and Cenozoic sedimentary rocks with typical Central Iranian stratigraphic features; and (ii) southwestern region (Shahrekord-Dehsard Terrane), which is an intensively faulted zone consisting of high- to low-grade metamorphic rocks and meta sedimentary strata with intercalations of intermediate to basic volcanic rock.

This terrane has been regarded as an old Precambrian basement (Taraz, 1974), reactivated in the course of the Mesozoic Cimmerian Orogeny (Gasemi & Hosaini, 2007). The boundary separating the southwest and the northeast regions is a major fault which Taraz (1974) was the first to name as the Main Deep Fault. Study area is situated in Shahrekord-Dehsard terrain. This sub-zone is distinguished from the other sub-zones by the abundance of metamorphic rocks. These rocks metamorphosed in greenschist facies and is Triassic to Jurassic age (Fig. 2). Schist, marble, amphibolites, quartzite, meta dolomite, and meta sandstone are the main constituents. Metamorphic conditions of these rocks are not well constrained. Earlier reports of Hercynian and older orogenies in Paleozoic rocks of the southeast complexly Deformed Sub-zone have been disputed by Alavi(1994) and most of the orogenic activity in the Sanandaj-Sirjan Zone is now related to closing of the Tethys. A large part of the Complexly Deformed Sub-zone consists of metamorphosed Mesozoic clastic, carbonate and some volcanic rocks. Subduction of Tethys under the marginal and Complexly Deformed Sub-zones has occurred to form a continental margin magmatic arc (Urumieh-Dokhtar Magmatic Arc) and associated plutonism, deformation and metamorphism (Davoudian *et al*, 2005). The studied area is a large-scale ductile shear zone trending NW–SE nearly parallel to the Main Zagros Reverse. Rocks are have undergone mylonitization causing mylonitic foliation and lineation. This area is characterized by the predominance of metamorphic rocks of both sedimentary and magmatic origins that are intruded by deformed granitoid bodies.

The metamorphic rocks are Triassic-Jurassic age and constitute an assemblage of low grade metamorphic that have been affected by several tectono-metamorphic events (Nasr-Esfahani & Ziaei, 2007). Davoudian *et al*. (2008) reported eclogites and other metamorphosed volcanic rocks in north Shahrekord, they suggest that these rocks represent relics of the Neo-Tethys oceanic plate, which was subducted under the Iranian micro continent. This area is near north

Shahrekord and geologically, the two regions are similar. In study area, metamorphic rocks are dominated by paragneisses, greenschists, meta volcanic, meta carbonates, which are intruded by granites (Davoudian *et al*, 2005). The meta basites are important metamorphic rocks that which are assumed to be oceanic plate remains, these rocks are the focus of the present study, and may reveal important information on tectonic setting of the Sanandaj-Sirjan Zone in this area. The aim of this paper is study petrogenesis of Mafic Meta volcanic Rocks in NW Isfahan, Central Iran and determine tectonic environment in this area.

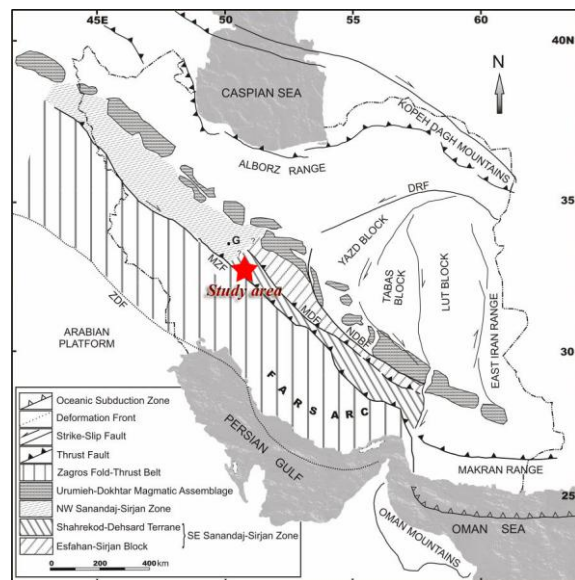


**Fig. 1.** Simplified structural map of Iran (compiled from (Gasemi & Hosaini, 2007)).

DRF, Darouneh Fault; G, Golpaygan city; MDF, Main Deep Fault; MZF, Main Zagros Fault, NDBF, Naien-Dehshir-Baft Fault; ZDF, Zagros Deformation Front.

## Materials and methods

### Area under study

The study area belongs to Shahrekord-Dehsard terrain in the north west of Isfahan and is underlain by various rocks ranging in age from Triassic to Quaternary. This area is located in 70 km NW of Isfahan, Central Iran (Fig. 1, 2). The lower most rock units in this area constitute Triassic-Jurassic metamorphosed igneous rocks which include meta basic rocks associated with greenschist and cut by doleritic dykes (Nasr-Esfahani & Ziaei, 2007).

Jurassic sedimentary rocks consist of shale and sandstone alternation with inter bedded limestone and dolomite (J1 and J2) over lie meta volcanics and greenschists, contact is sharp but conformable (Eliasi *et al*, 2011). These rocks developed over the greater part of the study area. Jurassic rocks are intruded by deformed granitoid body. This granite shows weaker metamorphic effects and they are strongly deformed during subsequent deformation events (Nasr-Esfahani & Ziaei, 2007). Cretaceous rocks are represented by marine carbonate and terrigenous-carbonate facies which rest with an angular unconformity on Jurassic underlying rocks and crop out in the north-east of area (Nasr-Esfahani & Ziaei, 2007, Eliasi *et al*, 2011).

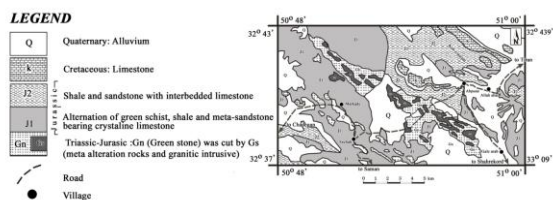


**Fig. 2.** Geological location of study area (modified from (Gasemi & Hosaini, 2007)).

#### Sampling and Analytical techniques

A total of 68 relatively fresh samples were selected from the metavolcanics rocks of the study area. The samples were deformed and metamorphosed under at least greenschist facies conditions. As a result, metamorphic minerals replaced igneous minerals, and deformational fabrics are pronounced. 6 samples after microscopy study were analyzed for major, trace and rare earth elements (REE) in the ALS Chemex analytical laboratory (Vancouver, Canada) by using ICP-MS (inductively coupled plasma mass spectrometry) after acid decomposition (Table 1). Major elements were determined by ICP-MS (inductively coupled plasma atomic emission spectrometry). Major element detection limits are about 0.001-0.2%. 4 samples (A.13, A.16, A.20.B, and L. 20)

were analyzed for major and minor elements by X-ray fluorescence spectrometry at the Laboratory of Isfahan University, Iran.

## Results and discussions

### Petrography

The meta-magmatic rocks are meta volcanics and dolerite dykes. They crop out south Ab-Puneh village. The meta-magmatic rocks are variably foliated. They are greenish in hand specimen due to dominance of chlorite and green amphibole (Fig. 3a). They contain tremolite- actinolite, epidote, chlorite mineral paragenesis that is indicative for low-grade metamorphism.

Metavolcanics are mainly fine to medium grained rocks, which commonly contain actinolitic amphibole, quartz, opaque minerals, and plagioclase porphyroblasts/ phenocrysts (Fig. 3b). Also, these minerals along with other mineral phases variably constitute the groundmass. The amphibole schist samples do not show any relict minerals and contain trace plagioclase and recrystallized quartz aggregates in the groundmass. Plagioclase with lamellar twinning and amphiboles are the dominant phenocryst phases in the meta basalt and greenschist outside. In meta basalts, igneous texture (ophitic/ subophitic) and mineralogy (partially replaced pyroxenes, saussuritized plagioclase) are locally preserved. Also, completely replaced plagioclase and pyroxene are locally traceable in greenschists. Alterations are intense in some of the meta volcanic samples from shear zones. Secondary minerals include epidote, chlorite, carbonate and sericite.

### Bulk sample geochemistry

Results of whole-rock geochemical analysis of all samples are presented in Table 1. The metavolcanic samples display  $\text{SiO}_2$ ,  $\text{Al}_2\text{O}_3$ ,  $\text{K}_2\text{O}$  and  $\text{MgO}$  contents ranging from 44.2 to 54.54, from 14 to 16.85, from 0.28 to 0.8 and from 2.55 to 10.55wt% respectively. The metavolcanic rocks are basic to intermediate in composition with  $\text{SiO}_2$ wt ranging from 44.2 to 54.54. However, most samples have  $\text{SiO}_2$  below 51% and high  $\text{MgO}$  (>6%) indicating the predominance of modestly fractionated basalts in the series. On the base of geochemical diagrams,  $\text{Zr}/\text{TiO}_2 \cdot 10^{-4}$  vs.  $\text{Nb}/\text{Y}$  diagram (Winchester & Floyd, 1977)(Fig. 4a),

the samples plot in the basalt field of this diagram. They show low Nb/Y ratio indicating subalkaline affinities (Fig.4b). This diagram is preferred to the more commonly used total-alkali-silica (TAS) classification diagram (Le Bas *et al*, 1986) as there may have been mobility of K in some of the more altered samples.

The total alkali content is low and K<sub>2</sub>O is lower than Na<sub>2</sub>O indicating a low-K and Fe-enriched tholeiitic nature. Tholeiitic trend is clearly indicated on the AFM diagram (Fig. 5a). Na<sub>2</sub>O+K<sub>2</sub>O vs. Al<sub>2</sub>O<sub>3</sub> diagram (Irvin & Baragar, 1971); the meta volcanic is dominated by sub-alkaline tholeiitic affiliation with moderate to high-Al basalts (Fig. 5b).

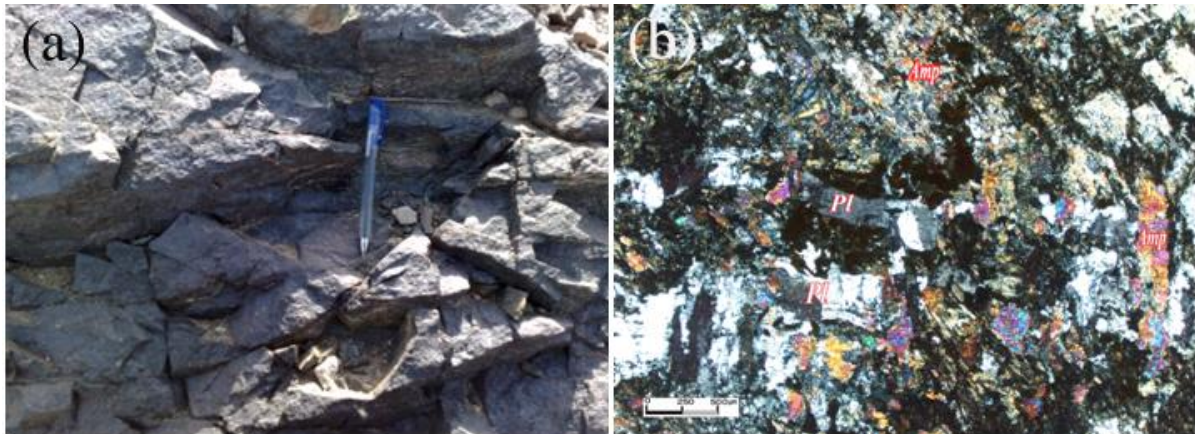


**Fig. 3.** Hand specimen (a) and microphotograph (b) of meta volcanics (Pl-plagioclase, Amp-amphibole).

**Table 1.** Major (Oxides: %wt) and trace elements (in ppm) data for meta volcanic rocks in study area.

Sample	K5	K10	K12	K12-1	K18	K20	A.13	A.16	A.20.B	L.20
<b>Major elements (Wt %)</b>										
SiO <sub>2</sub>	44.2	51.7	46.7	45.4	46.2	48.5	50.091	46.78	54.54	45.071
Al <sub>2</sub> O <sub>3</sub>	14	15.55	14.4	14.5	16.85	14.9	10.83	15.49	14.1	14.37
Fe <sub>2</sub> O <sub>3</sub> T	17.7	13.15	14.35	14.95	10.3	12	11.98	10.96	7.72	10.131
CaO	9.82	7.58	10.85	10.8	9.27	9.82	10.14	10.32	4/93	9/121
MgO	6.12	2.55	6.66	6.15	10.55	6.42	6.162	3.138	9.291	8.674
Na <sub>2</sub> O	2.3	4.41	2.64	2.43	2.16	1.64	1.603	3.223	3/069	2/267
K <sub>2</sub> O	0.39	0.6	0.67	0.52	0.28	0.73	0.62	0.53	0/8	0/64
Cr <sub>2</sub> O <sub>3</sub>	0.03	0.13	0.06	0.08	0.83	0.06	....	....	....	....
TiO <sub>2</sub>	3.69	1.8	2.23	2.32	0.78	1.5	1.26	2.069	0/637	0/984
MnO	0.25	0.18	0.27	0.26	0.18	0.21	0.206	0.135	0/084	0/146
P <sub>2</sub> O <sub>5</sub>	0.19	0.74	0.2	0.07	0.1	0.17	0.215	0.378	0/212	0/233
SrO	0.02	0.04	0.04	0.04	0.03	0.02	....	....	....	....
BaO	0.01	0.02	0.03	0.02	0.01	0.01	....	....	....	....
LOI	1.77	1.46	1.55	2.25	2.36	2.37	6.58	6.67	5/020	8/40
Total	100.49	99.91	100.65	99.79	99.9	98.4	99.687	99.693	100.603	99.674
Zr/Nb	8.75	31.66	6.84	17.5	18.52	17.21	13.11	9.63	12.45	19
Zr/Y	2.03	3.06	2.09	1.49	3.42	3.21	3.28	3.21	7.61	3.96
La/Nb	0.8	4.21	1.29	1.83	1.74	1.31	0.44	0.63	0.27	1
Th/Ta	0.63	6.75	2.78	1.8	2.4	2.42	....	....	....	....
Th/Yb	0.1	0.61	0.56	0.11	0.315	0.27	....	....	....	....
Ta/Yb	0.165	0.09	0.2	0.065	0.13	0.11	....	....	....	....
Nb/Y	0.23	0.096	0.31	0.85	0.185	0.186	0.25	0.33	0.61	0.21

Sample	K5	K10	K12	K12-1	K18	K20	A.13	A.16	A.20.B	L.20
Th/La	0.059	0.13	0.15	0.082	0.1	0.12	0.75	0.4	0.33	0
Ti/Zr	632.04	70.99	230.5	662.3	93.52	85.64	.....	.....	.....	.....
Mg#	40.9	28.07	48.11	45.16	67.17	51.61	.....	.....	.....	.....
FM	0.49	0.6	0.42	0.45	0.25	0.38	.....	.....	.....	.....
<b>Trace elements (ppm)</b>										
Au	<0.001	<0.001	<0.001	<0.001	<0.001	0.007				
Ag	<1	<1	<1	<1	<1	<1				
Ba	101.5	174	257	173	111.5	118.5	114	174	133	210
Co	51.3	19.7	30.5	32.7	53.1	41.9	46	28	29	42
Cr	210	900	430	570	5960	430	239	200	172	285
Cs	0.48	0.22	0.51	0.47	1.2	0.5				
Cu	48	14	21	25	69	114	91	62	5	53
Ga	19.9	26.2	20.5	18.5	15.3	18.3				
Hf	1	3.9	1.8	0.7	1.4	3				
Mo	<2	2	<2	<2	<2	<2				
Nb	4	4.8	8.6	1.2	2.7	6.1	9	8	11	5
Ni	24	11	76	33	186	51	49	9	39	157
Pb	9	10	12	11	26	20	29	46	13	15
Rb	11.1	12.3	13.1	10	7	34.7	30	18	33	28
Sn	<1	3	1	<1	1	1				
Sr	188.5	312	331	278	207	167	184	285	266	254
Ta	0.3	0.4	0.6	0.1	0.2	0.4				
Th	0.19	2.7	1.67	0.18	0.48	0.97	3	2	1	0
Tl	<0.5	<0.5	<0.5	<0.5	<0.5	<0.5				
U	0.1	0.99	0.79	0.08	0.14	0.36	4	5	9	3
V	675	129	366	417	150	288	243	229	239	143
W	3	2	3	2	2	1				
Y	17.2	49.7	27.7	14.1	14.6	32.7	36	24	18	24
Zn	161	100	176	170	294	1040	1438	605	189	289
Zr	35	152	58	21	50	105	118	77	137	95
<b>Rare elements (ppm)</b>										
La	3.2	20.2	11.1	2.2	4.7	8	4	5	3	5
Ce	7.9	46.5	23.7	5.6	10.8	18.8				
Pr	1.27	6.64	3.18	0.93	1.54	2.85				
Nd	6.9	30.5	13.8	4.9	7.2	13.4				
Sm	2.22	7.94	3.68	1.66	1.96	3.86				
Eu	1.3	2.75	1.59	1.21	0.91	1.44				
Gd	2.74	9.04	4.31	2.03	2.37	4.68				
Tb	0.53	1.56	0.81	0.42	0.43	0.93				
Dy	3.44	9.29	5.33	2.88	2.77	6.42				
Ho	0.73	1.97	1.07	0.59	0.58	1.3				
Er	2.04	5.32	3.08	1.69	1.56	3.74				
Tm	0.28	0.74	0.45	0.24	0.26	0.54				
Yb	1.81	4.41	2.96	1.53	1.52	3.6				
Lu	0.27	0.69	0.43	0.24	0.22	0.54				

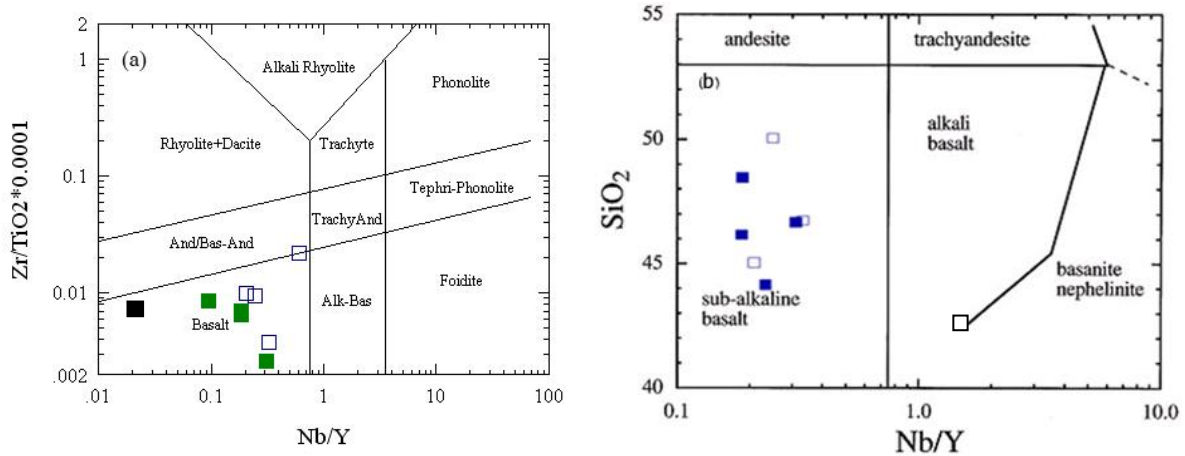


**Fig. 4.** Classification of magma types(a) ,Zr/TiO<sub>2</sub> \*10<sup>-4</sup> vs. Nb/Y diagram(Winchester & Floyd, 1977) for meta volcanic. SiO<sub>2</sub> versus Nb/Y[18].( ICP-MS samples & X-ray samples)

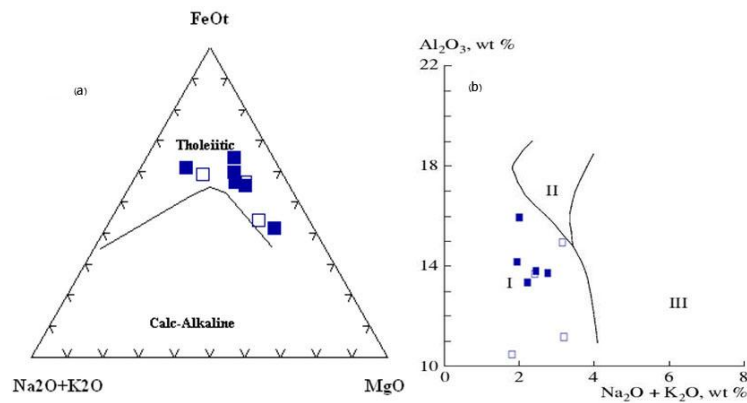


**Fig. 5.** The meta volcanic samples plot in sub-alkaline field. Classification of the studied rocks on (a) AFM (Irvine & Baragar, 1971), (b) Na<sub>2</sub>O+K<sub>2</sub>O vs Al<sub>2</sub>O<sub>3</sub> diagram (Kuno, 1961) for the meta volcanic rocks. Fields: I-tholeiitic, II-aluminous basalts, III-alkaline basalts. Symbols are the same as in Fig. 3.

*Trace and rare earth elements (REEs)*

In general, the chondrite normalized REE patterns of all meta volcanic rocks are characterized by moderate to high LREE enrichment [(La/ Yb)<sub>N</sub> = 1.17–3.05] and unfractionated HREE [(Gd/Yb)<sub>N</sub> = 1.04-1.63]. The meta volcanic rocks exhibit similar chondrite-normalized and primitive mantle-normalized REE patterns (Fig.6a and b).The E-MORB normalized spider diagrams of the met volcanic rocks were more similar to E-MORB (Fig. 6c). The Oceanic Island Basalt normalized patterns of these rocks are characterized by moderately fractionated REE with enrichment in HREE and depletion in LREE.(Fig. 6d).

Sampling rocks are normalized to Chondrite and primitive mantle (Rollinson, 1993), (Fig.7a, b) Rocks

are enriched in LILE (e.g. Ba and Pb), relatively depleted in HFSE (e.g., Ni, Ti). Well-defined negative anomaly is observed for Ni. Fractionation or presences of some minerals in the restates explain the negative anomalies, for example, olivine (Ni) and limonite and/or titanite (Ti).normalized to an average E- type MORB composition of the meta volcanic, show similarities and most of the samples have upper HFSE and LILE contents than Oceanic Island Basalt (Sun & Mc Donough, 1989), Fig.7.c.d). Meta volcanic have high Ba/ Nb (>28) ratios which is a common feature of arc magmas (e.g. Fitton, 1991)) and high La/Nb ratios (0.27-4.21) indicating crustal involvement (Hasse *et al*, 2000). Further, prevalent low Ce/Pb and Rb/Ba values also suggest lithospheric contributions.

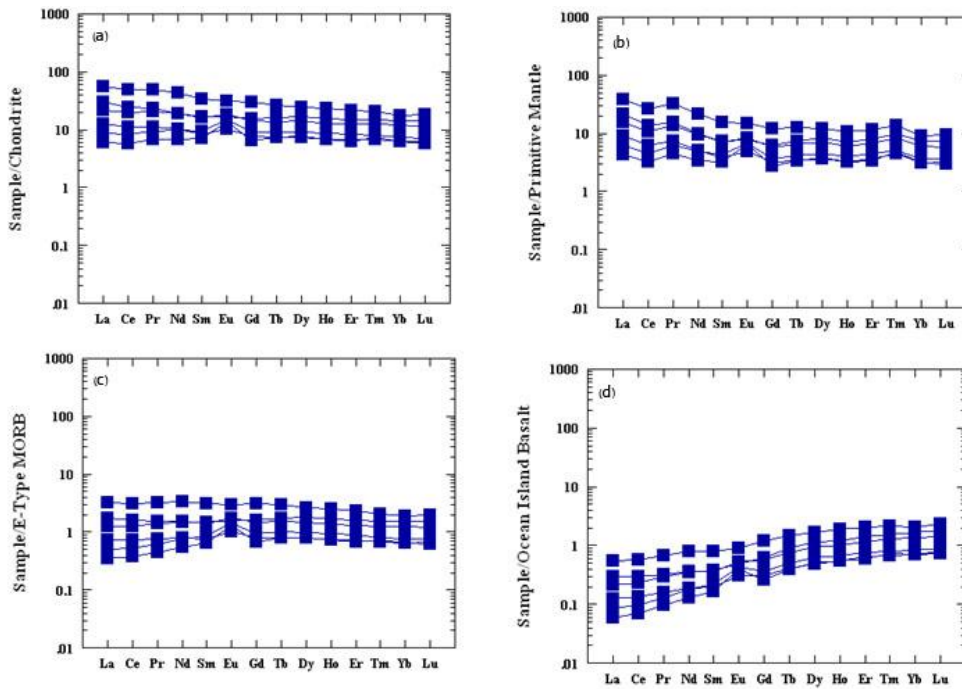


**Fig. 6.** (a) Chondrite-normalized REE pattern for meta volcanic rocks. (b) The meta volcanic rocks normalized with primitive mantle, Normalization data from (Taylor & McLennan, 1985). (c) E-type MORB-normalized. (d) Oceanic Island Basalt (normalized data from (Rollinson, 1993).

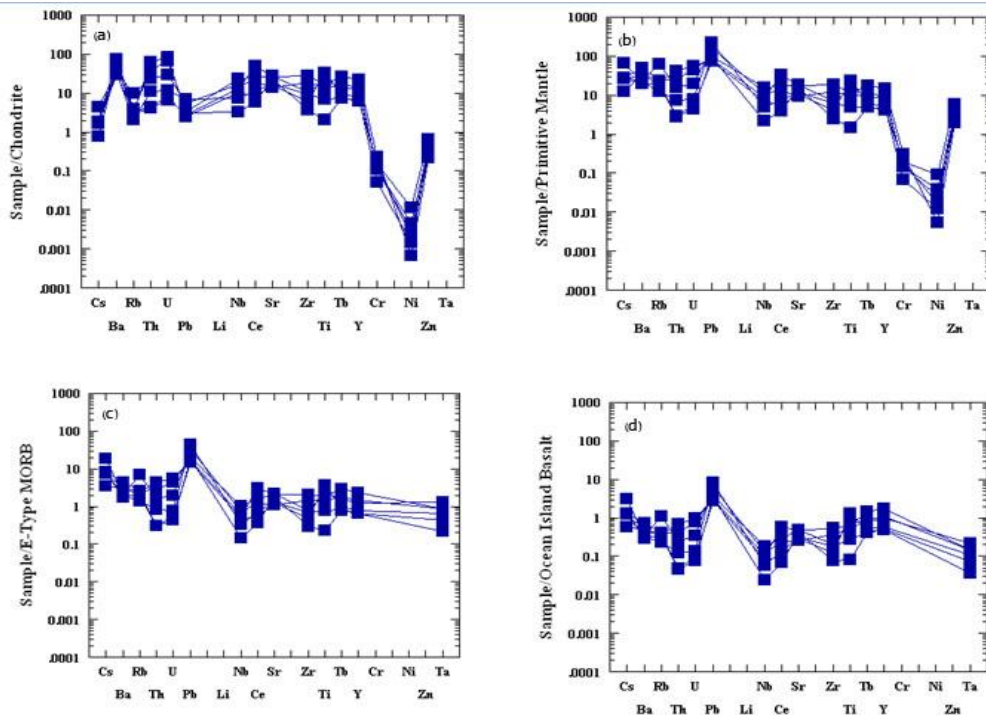


**Fig. 7.** Plate trace elements pattern (a) Chondrite-normalized, (b) primitive mantle (normalized data from (Taylor & McLennan, 1985), (c) E-type MORB-normalized, (d) Oceanic Island Basalt (normalized data from Rollinson, 1993).

*Tectonic setting*

Tectonic discrimination on Y, Zr and Ti triangular diagram (Pearce & Cann, 1973) shows that most sample plot on the ocean floor basalt fields (Fig. 8a).

The  $\text{CaO}/\text{TiO}_2$  and  $\text{Al}_2\text{O}_3/\text{TiO}_2$  ratios for the basic rocks from the meta volcanics are shifted towards lower values than most volcanic arc rocks (Fig. 8b) suggesting a source that is not similar to the source for the modern arc lavas (Sun & Nesbitt, 1978). Wilson (1989) has indicated that a contribution from the subducted component in terms of the highly incompatible elements such as Ti, Zr, Y and Nb is insignificant compared to the role from the asthenospheric mantle wedge above the subducted slab. Besides, the higher ratios of the incompatible elements with respects to average basalts from oceanic island-arcs and normal mid-oceanic ridges may indicate a contribution from an incompatible elements-enriched melt.

Within-plate basalts having higher Ti/Y and higher Nb/Y reflect an enriched mantle source relative to the source of MORB and volcanic arc basalts (Rollinson, 1993), the analyzed rocks plot in the plate-margin basalts, indicating enrichment in Zr and Ti compared with Within-plate basalts (Fig. 8c). Zr/Y plotted against the fractionation index Zr (adapted from (Pearce & Norry, 1979) provided an effective discrimination between the basalts from ocean-island arcs, mid-ocean basalts, within-plate basalts and back-arc basin basalts (Rollinson, 1993), and the meta volcanic plot in the field of back-arc basin basalts (Fig. 8d). Back-arc basin basalts (BABB) have notably higher Zr, lower Ti/Zr, V/Ti and Sc/Y values than island arc basalts (IAB) (Wood head *et al*, 1993).

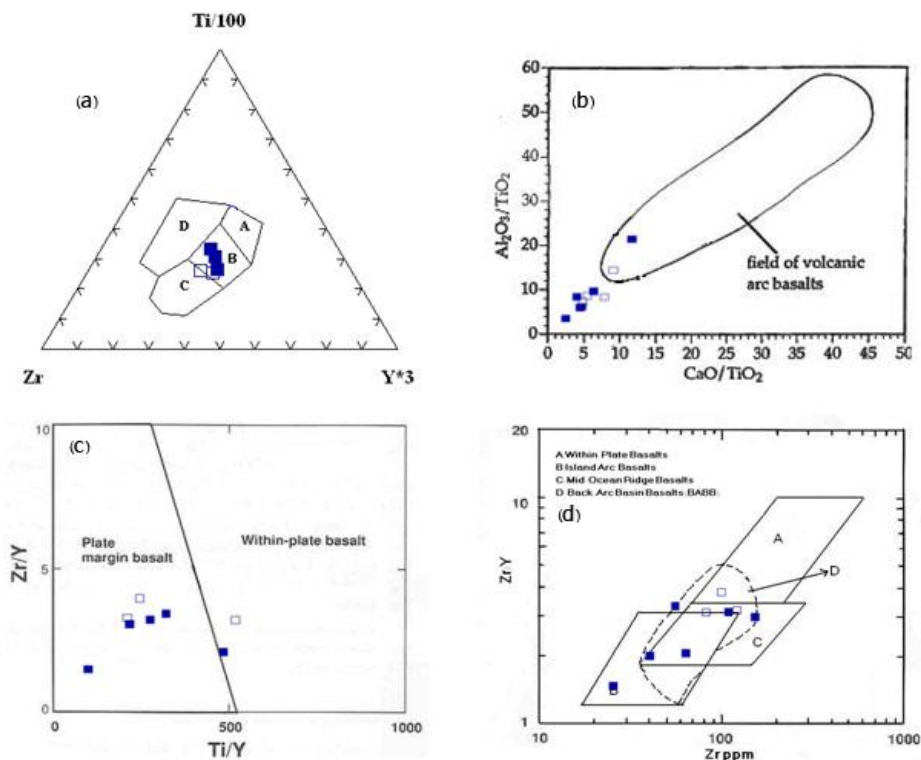


**Fig. 8.** Tectonic discrimination diagrams for meta volcanic on (a) Ti/100-Zr-3Y (Pearce & Cann, 1973). Tectonic discrimination on Y, Zr and Ti triangular diagram shows that most samples plot on the ocean floor basalt field, (b) Plots of the meta volcanic rocks on  $\text{CaO}/\text{TiO}_2$  versus  $\text{Al}_2\text{O}_3/\text{TiO}_2$  diagram (Sun & Nesbitt, 1978), (c) Zr/Y-Ti/Y diagram (Pearce & Gale, 1977), (d) Zr/Y-Zr diagram (Pearce & Norry, 1979); back-arc basalts discrimination from (Floyd *et al*, 1991) Symbols are the same as in Fig. 3.

A) Island arc basalts, B) Ocean floor basalts, C) Calc-alkaline basalts, D) Within plate basalts.

## Conclusion

According to this research, meta volcanics in the study area are basaltic composition with sub-alkaline and tholeiitic trend and indicated to the oceanic crust and were created in back arc basin environment. Chemically this rocks are as much enriched as N-type MORB and similar E-type MORB. Meta volcanic rocks are probably remnants of second Neo-Tethyan Oceanic crust with back arc basin environment. Arfania and Shahriari (Arfania & Shahriari, 2009) have showed that probably rifting and spreading jumped west to separated Shahrekord-Dehsardterrane from the north-eastern margin of the Afro-Arabian continent, creating the new Neo-Tethys (equal Neo-Tethys 2) in Trassic Jurassic time. This new plate was probably active by the end of Mesozoic time. I suggest that because of petrological and geochemical nature, meta volcanics represent relics of the Neo-Tethys oceanic plate, which was subducted under the Iranian microcontinent (as a part of Eurasia).

## Reference

- Agard P, Omrani J, Jolivet L, Mouthereau F.** 2005. Convergence history across Zagros (Iran): Constraints from coalitional and earlier deformation. *International Journal of Earth Sciences*. **94**, 401–419.
- Alavi M.** 1994. Tectonics of the Zagros Organic belt of Iran: New Data & Interpretations *Tectonophysics*. **229**, 211–238.
- Alavi M.** 2004. Regional stratigraphy of the Zagros fold-thrust belt of Iran and its proforeland evolution. *American Journal of Science*. **304**, 1–20.
- Arfania R, Shahriari S.** 2009. Role of southeastern Sanandaj-Sirjan Zone in the tectonic evolution of Zagros Orogenic Belt, Iran. *Journal of Island Arc*. **18**, 555–576.
- Babaie HA, Ghazi A M, Babaei A, Duncan R, Mahony J, Hassanipak A.** 2003. New Ar-Ar age, isotopic, and geochemical data for basalts in the Neyrizophiolite, Iran. *Geophysical Research Abstracts*. **5**, 812–899.
- Berberian M.** 1995. Master 'blind' thrust faults hidden under the Zagros folds: Active basement tectonics and surface morphotectonics. *Tectono physics*. **241**, 193–224.
- Davoudian AR, Genser J, Dachs E, Shahanian N.** 2008. Petrology of eclogites from north of Shahrekord, Sanandaj-Sirjan zone, Iran.
- Davoudian AR, Khalili M, Noorbehesht I, Mohajjel M.** 2005. The tectonometamorphic & magmatic evolution in the Shahrekord- Daranarea (Sanandaj-Sirjan Zone, Iran). Ph.D. thesis. University of Isfahan. 217.
- Eftekharnajad J.** 1981. Tectonic division of Iran with respect to sedimentary basins. *Journal of Iranian Petroleum Society*. **82**, 19–28 (in Farsi).
- Eliasi N, Emami N, Nasr-Esfahani AK, Vahabi Moghaddam B.** 2011. Mineralogy and determination of tectono magmatic setting of sub volcanic rocks in North of Shahrekord by using clinopyroxene mineral chemistry. **19(2)**, 207–218.
- Fakhari M D, Axen GJ, Horton BK, Hassanzadeh J, Amini A.** 2008. Revised age of proximal deposits in the Zagros foreland basin and implications for Cenozoic evolution of the High Zagros. *Tectonophysics*, **451**, 170–185.
- Fitton JG, James D, Leeman WP.** 1991. Basic magmatism associated with late Cenozoic extension in the western United States: compositional variations in space and time. *Journal of Geophysical Research*. **96**, 13693–13711.
- Floyd PA, Kelling G, Gokcen SL, Gokcen N.** 1991. Geochemistry and tectonic environment of basaltic rocks from the Misisophiolitic mélange, south Turkey. *Chemical Geology*. **89**, 263–280.
- Gasemi A, Hosaini M.** 2007. 1:100000 Geological map of Chadegan. Geological survey and mineral explorations of Iran.

- Ghasemi A, Talbot CJ.** 2006. A new tectonic scenario for the Sanandaj-Sirjan Zone (Iran). *Journal of Asian Earth Sciences.* **26**, 683–693.
- Hasse KM, Muhe R, Stoffers P.** 2000. Magmatism during extension of the lithosphere: geochemical constrains from lavas of the Shaban deep. *Northern Red Sea Chemical geology.* **166**, 225-239.
- Irvine TN, Baragar WRA.** 1971. A guide to the chemical classification of the common volcanic rocks. *Canadian Journal of Earth Science.* **8**, 523-548.
- Kuno H.** 1961. High Alumina Basalt. *Journal of petrology.* **1**, 121-145.
- Le Bas MJ, Le Maitre RW, Streckeisen A, Zanetin B.** 1986. A chemical classification of volcanic rocks based on the total alkalis- silica diagram. *J. Petrol.* **27**,745-750.
- Mohajjel M, Fergusson CL, Sahandi MR.** 2003. Cretaceous-Tertiary convergence and continental collision, Sanandaj- Sirjan Zone, Western Iran. *Journal of Asian Earth Sciences.* **21**,397-412.
- Mohajjel M, Fergusson CL.** 2000. Dextraltranspression in Late Cretaceous continental collision, Sanandaj - Sirjan zone, Western Iran. *Journal of Structural Geology.* **22 (8)**, 1125-1139.
- Mouthereau F, Tensi J, Bellahsen N, Lacombe O, De Boisgollier T, Kargar S.** 2007. Tertiary sequence of deformation in a thin-skinned/thick-skinned collision belt: The Zagros Folded Belt (Fars, Iran). *Tectonics.* **26**.
- Nasr-Esfahani AK, Ziaei HR.** 2007. Using multivariable statistical methods to separation and detection of lithologic units in ETM<sup>+</sup> satellite images, case study: outcrops in the south of Ab-Ponehvillage, Tiran (west Isfahan). *JSIAU.* **17(65)**, 27-42.
- Pearce JA, Cann JR.** 1973. Tectonic setting of basic volcanic rocks determined using trace element analyses. *Earth and Planetary Science Letters.* **19**, 290-300.
- Pearce JA, Gale GH.** 1977. Identification of ore deposition environment from trace element geochemistry of associated igneous host rocks. In *Volcanic Processes in OreGenesis* (Ed. M. J. Norry), Geological Society of London. **7**.
- Pearce JA, Norry MJ.** 1979. Petrogenetic implication of Ti, Zr, Y and Nb variation in volcanic rocks. *Contribution to Mineral and Petrology.* **69**, 33-47.
- Reuter M, Piller WE, Harzhauser M.** 2007. The Oligo-Miocene Qom Formation (Iran): Evidence for an early Burdigalian restriction of the Tethyan Seaway and closure of its Iranian gateways. *International Journal of Earth Science.* **98**, 627–650.
- Ricou LE.** 1974. L'étude géologique de la région de Neyriz (Zagros iranien) et l'évolution des Zagrides. Thesis. Université Paris-Sud. Orsay.
- Rollinson H.** 1993. Using geochemical data: evaluation, presentation, interpretation. Longman Scientific and Technical. **352**.
- Sengor MC, Natalin B A.** 1996. Paleotectonics of Asia: Fragments of a synthesis. In Yin A. & Harrison T. M. (eds.) *The Tectonic Evolution of Asia.* 486–640.
- Sepehr M, Cosgrove JW.** 2004. Structural framework of the Zagros Fold-Thrust Belt, Iran *Mar Petrol. Geology.* **21**, 829-843.
- Shafaii-Moghadam H, Rahgoshay M, Whitechurch H.** 2007. The Naïen-Baftophiolites: Anevidence of back-arc basin spreading in the activemargin of the Iranian continent. *Geophysical Research Abstracts.* **9**, 791.

**Shahabpour J.** 2007. Island-arc affinity of the Central Iranian Volcanic Belt. *Journal of Asian Earth Sciences*. **30**, 652–659.

**Sun SS, Mc Donough WF.** 1989. chemical and isotopic systematic of oceanic basalts: implication for mantle composition and processes. In: *Sunders, A. D. Norry, M.J(Eds.), Magmatic in Oceanic Basins, Special Publication. Geology Society of London.* **42**, 313–345.

**Sun SS, Nesbitt RW.** 1978. Geochemical regularities and genetic significance of ophiolitic basalts. *Geology*, **6**, 689-693.

**Taraz H.** 1974. Geology of the Surmagh- Deh Bid Area, Abadeh Region, Central Iran. Geological Survey of Iran. Tehran. 37.

**Taylor SR, Mc Lennan SM.** 1985. *The Continental Crust: its Composition and Evolution.* Blackwell, Cambridge. 312.

**Wilson M.** 1989. *Igneous Petrogenesis.* Unwin Hyman. London. 1– 46.

**Winchester JA, Floyd PA.** 1977. Geochemical discrimination of different magma series and their differentiation products using immobile elements. *Chemical of Geology*. **20**, 325-343.

**Woodhead J, Eggins S, Gamble J.** 1993. High field strength and transition element system in island arc back-arc basin basalts: evidence for multi-phase melt extraction and depleted mantle wedge. *Earth and Planetary Science Letters*. **114**, 491-504.